

# Supporting Information: Abnormal CO<sub>2</sub> and H<sub>2</sub>O Diffusion in CALF-20(Zn) Metal-Organic Framework: Fundamental Understanding of CO<sub>2</sub> Capture

Yann Magnin,<sup>\*,†</sup> Estelle Dirand,<sup>‡</sup> Guillaume Maurin,<sup>¶</sup> and Philip L. Llewellyn<sup>§</sup>

<sup>†</sup>*TotalEnergies, OneTech, R&D, CSTJF, Pau, 64018, France.*

<sup>‡</sup>*TotalEnergies, OneTech, Power R&D, Le Playground, Paris Saclay, 91400, France.*

<sup>¶</sup>*ICGM, Univ. Montpellier, CNRS, ENSCM, Montpellier, 34293, France*

<sup>§</sup>*TotalEnergies, OneTech, Sustainability R&D, CSTJF, Pau, 64018, France.*

E-mail: [yann.magnin@totalenergies.com](mailto:yann.magnin@totalenergies.com)

## Diffusion theory

In equilibrium bulk phase, thermal energy induces particle diffusion through Brownian's motion. For a single tagged particle, we can assess the self-diffusion coefficient  $D_s$ , depending on the fluid temperature and density.<sup>1</sup> Self-diffusion is accessible from different experimental techniques like NMR, QENS or IFM, and from the plot of the time dependence of the mean square displacement (MSD) simulated for a tagged particle.<sup>2,3</sup> MSD is based on Einstein's relationship, stating that the diffusion coefficient is given by the mean-square displacement

of molecules along time such as,

$$D_s = \frac{1}{2dN} \lim_{t \rightarrow \infty} \frac{d}{dt} \left\langle \sum_{i=1}^N (\mathbf{r}_i(t) - \mathbf{r}_i(0))^2 \right\rangle. \quad (1)$$

In (1),  $d$  is the dimension of the system,  $N$  the number of particles,  $r_i(t)$  the position of a particle  $i$  at time  $t$  and the angular brackets denote an ensemble average. For systems filled by molecules, the MSD increases linearly as a function of time due to molecules collisions and the average of the MSD slope allows to determine  $D_s$ , Figure S3A.

To account for collective interactions, corrected diffusion coefficient  $D_0$  can be expressed by different methods.  $D_0$  can be approached by MSD, while instead averaging each molecule positions, collective displacement is averaged from the fluid center of mass  $R$ . Thus, (1) can be expressed in its corrected form as follow,<sup>2</sup>

$$D_0 = \frac{N}{2d} \lim_{t \rightarrow \infty} \frac{d}{dt} \langle (\mathbf{R}(t) - \mathbf{R}(0))^2 \rangle. \quad (2)$$

However, this approach presents strong fluctuations and required larger number of long simulations compared to  $D_s$ .<sup>1</sup> Derivating (1), we can formulate the Green-Kubo equation (GK),

$$D_s = \frac{1}{dN} \sum_{i=1}^N \int_0^\infty \langle \mathbf{v}_i(t) \cdot \mathbf{v}_i(0) \rangle dt. \quad (3)$$

In (3), the dot product of velocities corresponds to the velocity auto-correlation function (VACF). In confined systems, the VACF presents an oscillating behavior, resulting from molecules collisions and molecules (back-)scattering due to their interactions with an adsorption site, Figure S3B.

It stems from the above that molecules are also more or less correlated with the motion of their neighbors and particles diffusion is thus a collective property writing in GK formalism as a sum of  $D_s$  (3) (first sum in (4)) and cross terms, integrating the velocity correlation

function (VCF) (second sum in (4)),

$$D_0 = \frac{1}{dN} \left\{ \sum_{i=1}^N \int_0^\infty \langle \mathbf{v}_i(t) \cdot \mathbf{v}_i(0) \rangle dt + \sum_{i \neq j}^N \int_0^\infty \langle \mathbf{v}_j(t) \cdot \mathbf{v}_i(0) \rangle dt \right\}. \quad (4)$$

In highly confined environments (pore sizes of few molecular diameters), molecules mostly interact with solid pore surfaces, while guest interactions or their coordination remains more or less limited. In such conditions, molecules behave almost independently and the cross term in (4) is negligible,  $D_s \sim D_0$  citefalk2015. If such an approximation can be made for confined and dilute media, a special care has to be made with dense media, for example water, that tends to form clusters in (sub-)nanopores. The GK is challenging method to be converged. It depends on the integration time step and time length, where the infinite limit in integrals has to be approximated and large ensemble average is required.

Transport diffusion (non-equilibrium dynamics)<sup>4</sup> presents an interesting alternative to equilibrium methods described above. In such a technique, flux of molecules is driven by the application of an external driving force. In the steady regime, the flux of molecules can be expressed as follow,

$$j = \rho \times v, \quad (5)$$

with  $j$  denoting the molecules flux,  $\rho$  the molecules density and  $v$  their velocities. Noting that the driving force initiating the molecules flow can be noted such as,

$$F = v \times f = -\nabla\mu, \quad (6)$$

where  $v$  is the fluid velocity,  $f$  the friction coefficient of fluid molecules and  $F = -\nabla\mu$  the driving force, expressed as a gradient of chemical potential. Noting that  $\mu = \mu_0 +$

$k_B T \ln(P/P_0)$  and coupling to (6), we can express the first Fick’s law,

$$j = -\frac{k_B T}{f} \frac{d \ln(P)}{d \ln(\rho)} \frac{d \rho}{d r} = -D_t \nabla \rho, \quad (7)$$

with  $D_t$ , the transport coefficient. From (7),

$$D_t = \frac{k_B T}{f} \frac{d \ln(P)}{d \ln(\rho)} = D_0 \times \Gamma, \quad (8)$$

with  $D_0$  the corrected diffusion coefficient and  $\Gamma$  the thermodynamic factor (Darken’s factor). For simulation purpose, (7) is reformulated with the driving force,  $-\nabla \mu$ . Noting that  $D_0 = k_B T/f$  and  $\nabla \mu/k_B T = \nabla \ln(P)$ , molecules velocity reads,

$$v = -\frac{D_0}{k_B T} \nabla \mu. \quad (9)$$

To determine  $D_0$  from NEMD simulations, we used (9), applying a constant force  $F = -\nabla \mu$  on the center of mass of guests molecules along one direction. During simulations, the center of mass velocity is average along time, and  $D_0$  can then be fitted has shown in Figure S4. It is important to note that the thermostat in molecular dynamics is turned off along the flow direction in order to not introduce a flow bias.

## Methods

All simulations have been made in a triclinic CALF-20 atomistic structure of  $4 \times 3 \times 3$  super-cells with REPEAT point charges proposed by Shimizu et al.,<sup>5</sup> Figure S1. Thermodynamics simulations (adsorption and isosteric enthalpy) has been calculated from Monte Carlo algorithm in the grand canonical ensemble (GCMC),<sup>6</sup> in which the MOF structure randomly exchanges molecules with an ideal gas reservoir kept at constant guests chemical potential  $\mu$ , volume  $V$  and temperature  $T = 293.15\text{K}$ . A cycle consists in trying 500 molecules insertions

or deletions, randomly chosen with 50% probability, followed by 5 ps relaxation by molecular dynamics. GCMC simulations were run for  $4 \times 10^4$  Monte Carlo cycles for CO<sub>2</sub> and  $1 \times 10^5$  for H<sub>2</sub>O adsorption. The first half cycles were used to equilibrate the system and remaining cycles were used for averaging guests density from equilibrium microstates.

GCMC simulations do not directly control the pressure, but the chemical potential,

$$\mu = k_B T \ln \left( \frac{f \Lambda^3}{k_B T} \right), \quad (10)$$

with  $\Lambda$  the de Broglie thermal wave length, and  $f$  the fugacity. The pressure is thus determined from  $f$ , whose form in Eq.10 depends on the ideal gas equation of state. In order to estimate the pressure, that may deviate from ideal gas under some thermodynamic conditions, fugacity has been corrected from the Soave-Redlich-Kwong (SRK) model.<sup>7</sup>

Inter-atomic parameters has been calculated from the Lorentz Berthelot mixing rule and can be found in lammmps inputs shared with this paper. The CO<sub>2</sub> and H<sub>2</sub>O parameters can be found in the work of Calero et al.<sup>8</sup> and Horn et al.,<sup>9</sup> respectively. Force field cut-off were fixed at 1 nm for the Lennard Jones parameters, and long range interactions were ensured by the Ewald summation with a precision of  $10^{-5}$ . MD simulations to determine diffusion coefficients from the mean square displacement and NEMD as well as Green-Kubo techniques were run in the  $(N,V,T)$  ensemble for 50 ns with a time step of 1 fs and each reproduced 5 times from different initial configurations. A Nose-Hoover thermostat were used to keep constant pressure and temperature during full simulations.

Binding energies presented in the article were determined from MD simulations in the  $(N,V,T)$  ensemble. Equilibrated structures from GCMC has been annealed during 10 ns, with a thermal ramp ranging from  $T=400\text{K}$  to  $10\text{K}$ , with a time step of 1 fs. Binding energies were then determined from instantaneous energy calculations in annealed structures and have been reproduced 5 times to gain a better averaging in  $E_b$ .

Table S1: CALF-20 UFF parameters.<sup>10</sup> The REPEAT charges were taken from the supplementary materials (Table S3) in Shimizu and co-worker publication.<sup>5</sup>

Atoms	Zn	N	O	C	H
$\sigma$ (Å)	2.4616	3.2607	3.1181	3.4309	2.5711
$\epsilon$ (kcal/mol)	0.124	0.069	0.06	0.105	0.044

Table S2: CALF-20 Dreiding parameters.<sup>11</sup> The REPEAT charges were taken from the supplementary materials (Table S3) in Shimizu and co-worker publication.<sup>5</sup>

Atoms	Zn	N	O	C	H
$\sigma$ (Å)	4.0447	3.2626	3.0332	3.473	2.8464
$\epsilon$ (kcal/mol)	0.055	0.077	0.096	0.095	0.015

Table S3: Parameters for adsorbates.

Atoms	$C_{CO_2}$	$O_{CO_2}$	$O_{H_2O}$	$H_{H_2O}$
$\sigma$ (Å)	2.745	3.017	3.16435	0.0
$\epsilon$ (kcal/mol)	0.05948	0.17023	0.16275	0.0
q	0.6512	-0.3256	-1.0484	0.5242

## LAMMPS Atomistic Configuration

Belonging the Supporting Information, a LAMMPS 3D atomistic configuration of the CALF-20(Zn) filled by both  $CO_2$  and  $H_2O$  was provided. This configuration corresponds to coadsorption at  $T=293.15K$  for  $P_{CO_2}=0.1$  bar and  $P_{H_2O}/P_0=0.6$ .

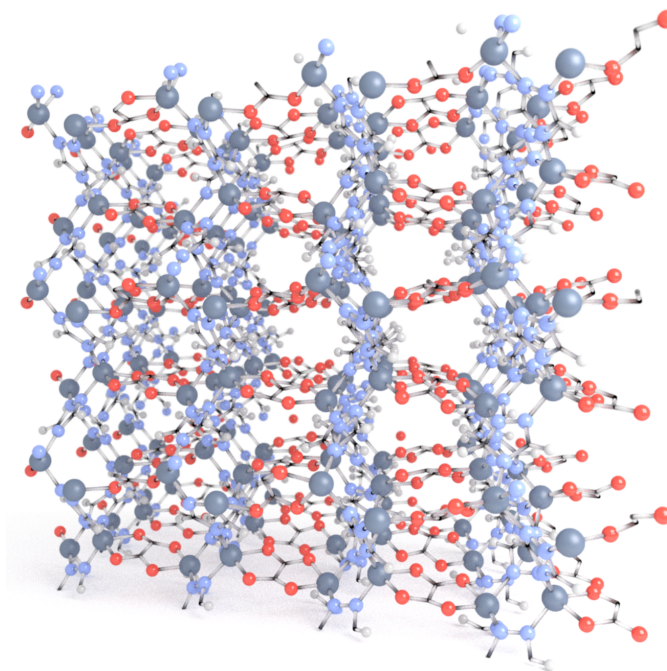


Figure S1: Atomistic structure of CALF-20 made of  $4 \times 3 \times 3$  super-cells. The CALF-20(Zn) structure is made of zinc oxide nodes, bridged by triazole and oxalate linkers with a resulting sub-nanoporous structure formed by cages with diameters of  $\sim 0.6 - 0.7$  nm and a surface area of about  $\sim 442$  m<sup>2</sup>/g.<sup>12</sup>

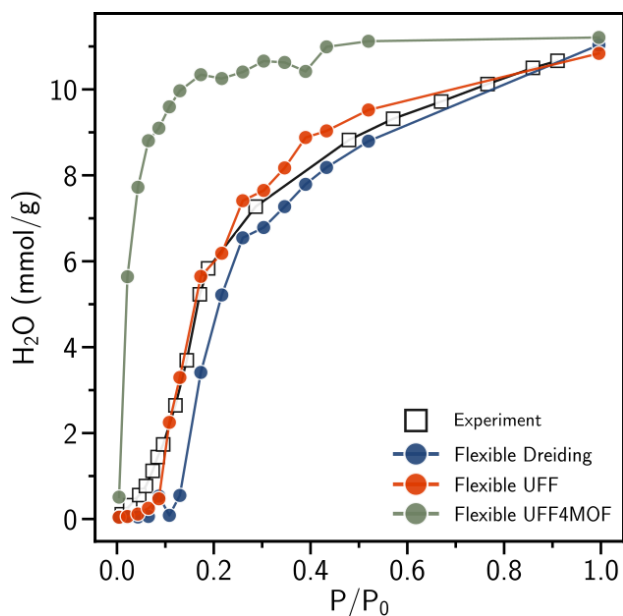


Figure S2: Water isotherms as a function of  $P/P_0$  at  $T=293.15$ K, determined from different CALF-20 force fields, UFF (orange), Dreiding (blue), UFF4MOF (green). Experimental data correspond to the open squares.

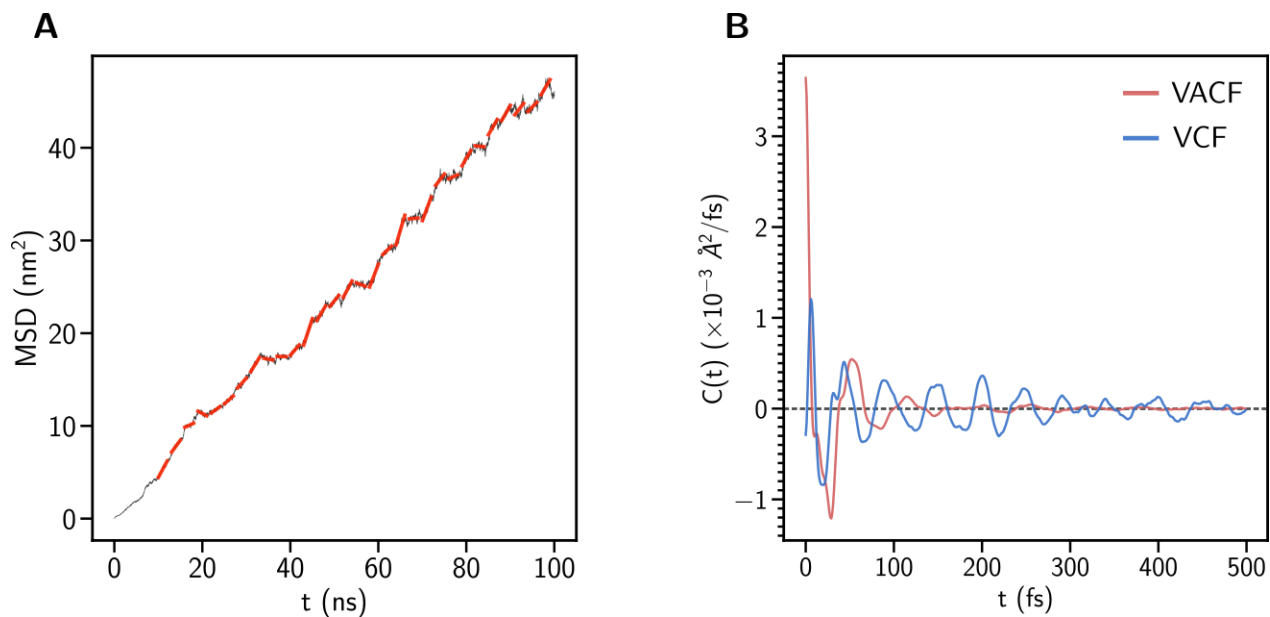


Figure S3: A. Mean square displacement of  $\text{CO}_2$  molecules at  $T=293.15\text{K}$  and  $P=1$  bar (black line) calculated from equilibrium MD. The red segments corresponds to fits of the MSD plot on short time scale. B. Velocity auto-correlations and velocity correlation of  $\text{CO}_2$  molecules at  $T=293.15\text{K}$  and  $P=1$  bar (red and blue lines, respectively).

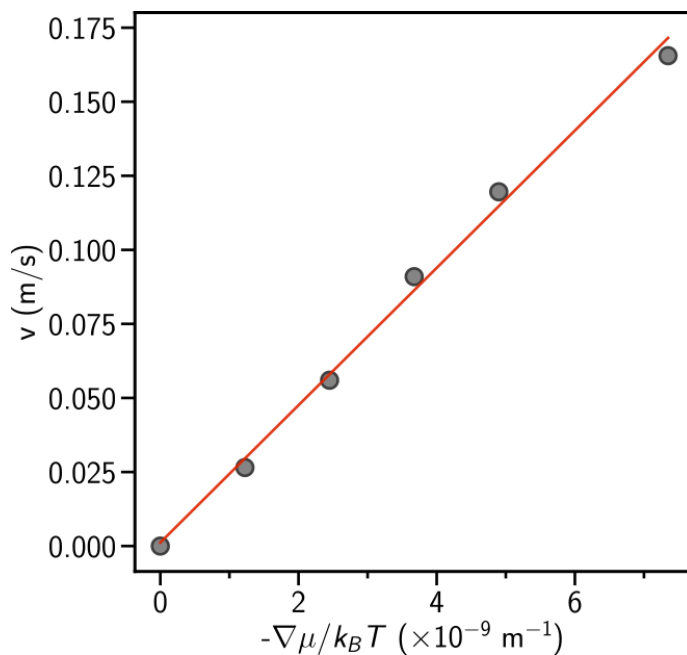


Figure S4: Velocity plotted as a function of different driving forces by out of equilibrium molecular dynamics (brown dots). The red line corresponds to the fit with a slope corresponding to  $D_0$ .



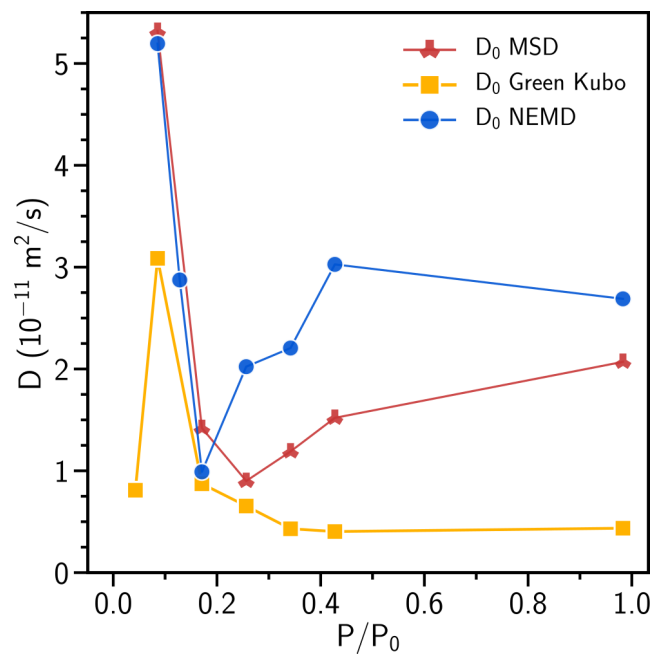


Figure S5: Corrected diffusion coefficient of water molecules in flexible CALF-20 by UFF force field using different methods. The red crosses corresponds to  $D_0$  from the MSD method, the yellow squares to the Green-Kubo approach and the blue circles to the NEMD technique. For a sack of clarity we remove error bars.

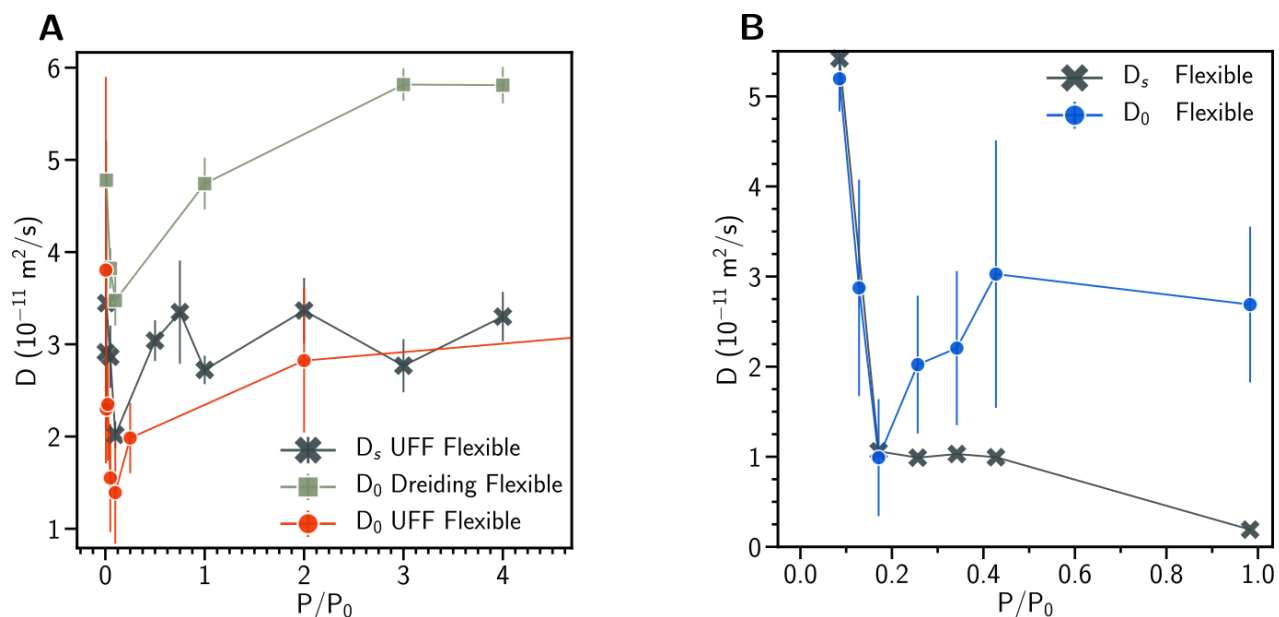


Figure S6: A. CO<sub>2</sub> diffusion coefficients in flexible CALF-20. The dark crosses correspond to the self-diffusion in a structure model by the UFF force field, determined by the mean square displacement method. The red circles to the corrected diffusion with the UFF force field and the green squares to the corrected diffusion with the Dreiding force field. The latter has been determined from non equilibrium technique. B. Full red circles correspond to the corrected diffusion coefficient in flexible CALF-20 from the UFF force field. Open circles corresponds to the corrected diffusion coefficient in a rigid MOF structure.

## References

- (1) Falk, K.; Coasne, B.; Pellenq, R.; Ulm, F.-J.; Bocquet, L. Subcontinuum mass transport of condensed hydrocarbons in nanoporous media. *Nature communications* **2015**, *6*, 6949.
- (2) Rouquerol, J.; Rouquerol, F.; Llewellyn, P.; Maurin, G.; Sing, K. S. *Adsorption by powders and porous solids: principles, methodology and applications*; Academic press, 2013.
- (3) Kaerger, J. Transport phenomena in nanoporous materials. *ChemPhysChem* **2015**, *16*, 24–51.
- (4) Frentrup, H.; Avendaño, C.; Horsch, M.; Salih, A.; Müller, E. A. Transport diffusivities of fluids in nanopores by non-equilibrium molecular dynamics simulation. *Molecular Simulation* **2012**, *38*, 540–553.
- (5) Lin, J.-B.; Nguyen, T. T.; Vaidhyanathan, R.; Burner, J.; Taylor, J. M.; Durekova, H.; Akhtar, F.; Mah, R. K.; Ghaffari-Nik, O.; Marx, S.; Fylstra, N. A scalable metal-organic framework as a durable physisorbent for carbon dioxide capture. *Science* **2021**, *374*, 1464–1469.
- (6) Frenkel, D.; Smit, B. *Understanding molecular simulation: from algorithms to applications*; Elsevier, 2001; Vol. 1.
- (7) Peng, D.-Y.; Robinson, D. B. A new two-constant equation of state. *Industrial & Engineering Chemistry Fundamentals* **1976**, *15*, 59–64.
- (8) García-Sánchez, A.; Ania, C. O.; Parra, J. B.; Dubbeldam, D.; Vlugt, T. J. H.; Krishna, R.; Calero, S. Transferable Force Field for Carbon Dioxide Adsorption in Zeolites. *The Journal of Physical Chemistry C* **2009**, *113*, 8814–8820.

- (9) Horn, H. W.; Swope, W. C.; Pitner, J. W.; Madura, J. D.; Dick, T. J.; Hura, G. L.; Head-Gordon, T. Development of an improved four-site water model for biomolecular simulations: TIP4P-Ew. *The Journal of chemical physics* **2004**, *120*, 9665–9678.
- (10) Rappé, A. K.; Casewit, C. J.; Colwell, K.; Goddard III, W. A.; Skiff, W. M. UFF, a full periodic table force field for molecular mechanics and molecular dynamics simulations. *Journal of the American chemical society* **1992**, *114*, 10024–10035.
- (11) Mayo, S. L.; Olafson, B. D.; Goddard, W. A. DREIDING: a generic force field for molecular simulations. *The Journal of Physical Chemistry* **1990**, *94*, 8897–8909.
- (12) Wei, Y.; Qi, F.; Li, Y.; Min, X.; Wang, Q.; Hu, J.; Sun, T. Efficient Xe selective separation from Xe/Kr/N<sub>2</sub> mixtures over a microporous CALF-20 framework. *RSC advances* **2022**, *12*, 18224–18231.